# Riluzole does not ameliorate disease caused by cytoplasmic TDP-43 in a mouse model of amyotrophic lateral sclerosis

Amanda L. Wright[1], Sheng Le[1], Prachi Mehta[1], Paul Della Gatta[2], Britt A. Berning[1,3], Kelly R. Jacobs[1], Hossai Gul[1], Rebecca San Gil[1,3], Thomas J. Hedl[1,3], Winonah R. Riddell[1], Owen Watson[1], Sean S. Keating[3], Roger S. Chung[1], Julie D. Atkin[1], Albert Lee[1], Bingyang Shi[1], Catherine A. Blizzard[4], Marco Morsch[1], Adam K. Walker[1,3]

[1]Centre for Motor Neuron Disease Research, Department of Biomedical Sciences, Faculty of Medicine and Health Sciences, Macquarie University, Sydney, NSW, Australia

[2]Institute for Physical Activity and Nutrition (IPAN), School of Exercise and Nutrition Sciences, Deakin University, Burwood, VIC, Australia

[3]Neurodegeneration Pathobiology Laboratory, Queensland Brain Institute, University of Queensland, Brisbane, QLD, Australia

[4]Menzies Institute for Medical Research, College of Health and Medicine, University of Tasmania, Hobart, TAS, Australia

Corresponding author: Dr Adam K. Walker (adam.walker@uq.edu.au)

Running title: Riluzole treatment in TDP-43 mice

Keywords: amyotrophic lateral sclerosis (ALS), TDP-43, motor neuron disease (MND), riluzole, glutamate receptors

**Abstract**

Amyotrophic lateral sclerosis (ALS) is a neurodegenerative disease most commonly treated with riluzole, a small molecule considered to act at least in part via modulation of glutamatergic neurotransmission. However, riluzole affords only a modest extension of lifespan for people living with ALS and its precise mechanisms of action remain largely unclear. Likewise, the vast majority of ALS cases are characterised by the pathological accumulation of cytoplasmic TDP-43, but the effects of riluzole in an *in vivo* model of ALS with disease-reminiscent TDP-43 pathology have not been thoroughly studied. We therefore tested the effects of daily riluzole treatment on TDP-43 pathology and disease onset and progression in transgenic mice that inducibly express nuclear localisation sequence (NLS)-deficient human TDP-43 in neurons of the brain and spinal cord (*NEFH*-tTA/*tetO*-hTDP-43ΔNLS, 'rNLS', mice). We found that treatment of rNLS mice with riluzole beginning from the first day of hTDP-43ΔNLS expression failed to alter disease onset, disease-associated weight loss or performance on multiple motor behavioural tasks over a 6-week period. Riluzole treatment also did not alter soluble or insoluble TDP-43 protein levels or TDP-43 phosphorylation in rNLS mice. By quantifying levels of key proteins involved in glutamatergic signalling, we identified a dramatic loss in GluA3 protein in the rNLS mice after disease onset, however riluzole was unable to ameliorate this disease-associated molecular phenotype. Finally, we assessed the ability of riluzole to affect disease in a long-term post-disease onset study in rNLS mice, and found that riluzole similarly had no effect on progression of late-stage disease or animal survival. Together, our findings demonstrate that the rNLS mouse model recapitulates glutamatergic receptor alterations reminiscent of ALS, but the approved ALS therapeutic riluzole has no effect on disease phenotypes in these animals. These studies suggest that strategies directly targeting disease-relevant pathways, such as accumulation of TDP-43 pathology, may be needed for development of more effective ALS treatments.

## Introduction

Amyotrophic lateral sclerosis (ALS) is a debilitating and inevitably fatal neurodegenerative disease causing paralysis due to progressive loss of upper and lower motor neurons of the brain and spinal cord (*1*). The small molecule 2-amino-6(trifluoromethoxy)benzothiazole, known generically as riluzole, is the most widely prescribed and until recently was the only approved drug therapy for the treatment of ALS (*2, 3*). However, the efficacy of riluzole is limited, resulting in a short extension in lifespan for people with ALS of only a few months, with little if any individual improvement in quality of life (*2, 4*). A better understanding of the biological mechanisms of ALS is needed, and determining the pathways through which riluzole exerts its modest effects may also aid the development of more effective therapeutics.

The mechanisms of action of riluzole remain unclear despite decades of use of this drug in people, although modulation of glutamatergic neurotransmission is likely involved (*5*). Indeed, people with ALS have increased levels of the excitatory neurotransmitter glutamate in cerebrospinal fluid (CSF) (*6*), and altered excitability of motor neurons may be an early feature of disease (*7, 8*). Amongst a myriad of other potential disease-relevant effects of riluzole, the drug has also been proposed to affect estradiol transport (*9*), to inhibit kinases potentially involved in ALS pathology (*10*), and to decrease activation of the heat shock response related to protein aggregation (*11*).

Although riluzole was shown to have a modest protective effect in early, small studies of the most widely used mouse model of ALS, the SOD1$^{G93A}$ mouse (*12, 13*), a later rigorous study demonstrated conclusively that SOD1$^{G93A}$ mice do not benefit from riluzole treatment (*14*). Likewise, in this and other mouse models of ALS expressing a rare ALS-linked TAR DNA binding protein of 43 kDa (TDP-43) mutant protein or a fused in sarcoma (FUS) model of disease, riluzole also failed to show any protective effect in function or lifespan of the animals (*15*). However, the hallmark pathology in the vast majority of ALS cases is cytoplasmic accumulation of non-mutated but post-translationally modified TDP-43 in affected regions of the brain and spinal cord (*16, 17*), and none of these previously studied mouse models recapitulate this key pathological feature of ALS. It therefore remained unclear

whether riluzole may be effective in a mouse model more closely resembling human ALS, which could illuminate differences between drug responses in mice and humans.

Here we sought to investigate the therapeutic effects of riluzole in a well-characterised mouse model with cytoplasmic accumulation of TDP-43, the *NEFH*-tTA/*tetO*-hTDP-43ΔNLS ('rNLS' mice), which more closely recapitulates the key pathology observed in the vast majority of people with ALS (*18*). We found that riluzole was unable to delay onset or alter progression of disease in rNLS TDP-43 mice when drug treatment began prior to symptom onset, in a study of the effects of riluzole in early disease. Similarly, riluzole treatment did not affect disease progression or survival of rNLS TDP-43 mice when drug treatment began after functional decline, in a study that more closely mimics the commencement of riluzole treatment after disease onset in people with ALS. Interestingly, we identified a significant decline in protein levels of the key glutamatergic α-amino-3-hydroxy-5-methyl-4-isoxazolepropinionic acid (AMPA) receptor subunit GluA3 in the rNLS TDP-43 mice, suggesting disease-related alterations in postsynaptic glutamate signalling, however riluzole afforded no protection against this change. Likewise, riluzole did not affect levels of soluble, insoluble or phosphorylated TDP-43, demonstrating a lack of efficacy in targeting the underlying pathology of disease. Overall, our findings show that riluzole has no effect on pathological changes or disease onset, progression or survival in the rNLS TDP-43 mouse model and provide additional impetus for identification of improved therapeutics for ALS.

## Materials and Methods

### *Animals*

Studies were approved by Macquarie University Animal Ethics Committee and adhered to the Australian code for the care and use of animals for scientific purposes. Transgenic TDP-43 rNLS mice for expression of human TDP-43ΔNLS were bred at Australian BioResources (Moss Vale, Australia) under specific pathogen-free conditions. Monogenic B6;C3-Tg(NEFH-tTA)8Vle/J (*NEFH*-tTA line 8, stock #025397) mice and monogenic B6;C3-Tg(*tetO*-TARDBP*)4Vle/J (tetO-hTDP-43ΔNLS line 4, stock #014650) mice were initially obtained from the Jackson Laboratory (Bar Harbour, ME, USA). Both lines were maintained individually on a mixed B6/C3H background by mating of monogenic male mice of each line to wildtype B6/C3H F1 females, which were obtained by the cross of female C57BL/6JArc mice with male C3H/HeJArc mice (Australian Resources Centre, Canning Vale, Australia). Generally, male *NEFH*-tTA mice were crossed with female *tetO*-hTDP-43ΔNLS mice to obtain bigenic TDP-43 rNLS and monogenic and non-transgenic littermate control mice.

### *Animal experiments overview*

Mice were transferred to and housed in the Central Animal Facility at Macquarie University for experiments. Mice arrived at least one week prior to beginning of experiments to allow for acclimatisation. For all therapeutic efficacy studies, littermates were used and allocated randomly by personnel independent from authors and experimenters to receive either vehicle or riluzole treatment in a double blinded manner. Experimenters were blinded to treatment but not to genotype. A small cohort of male TDP-43 rNLS mice were included in the study initially but were excluded from the dataset due to unforeseen complication of urinary retention as some of the mice aged. To avoid this confound, all mice outlined in this study were females. All animals were housed under identical conditions in a 12-hour standard light/dark cycle with access to water and food *ad libitum*. TDP-43 rNLS bigenic mice were housed together with matched littermate control mice. All breeding and weaned mice were fed a chow diet containing 200 mg/kg doxycycline (dox, Gordon Specialty Feeds). hTDP-43ΔNLS expression was induced in mice at 6-8 weeks of age by switching all mice to a matched standard chow diet lacking dox (Gordon Specialty Feeds). All mice were supplied with supplementary diet (DietGel 76A, Clear$H_2O$) from day 15 after switching to the standard diet.

### *Drug administration*

Riluzole (2-Amino-6-(trifluoromethoxy)benzothiazole, #R116-500mg, Sigma Aldrich) was dissolved into corn oil (C8267, Sigma Aldrich) to a final concentration of 3 mg/mL. For each treatment, either riluzole (volume calculated based on a dosage of 8 mg/kg) or the equivalent volume of corn oil (vehicle control) were gavaged once per day into the stomach of the mice using a flexible feeding tube (FTP-20-38, Instech Laboratories, Inc). Treatment was started on day 0 (for onset study) or on day 29 (for post-onset study) of switching to the standard diet. All drug treatments were given once daily (between 0900h – 1200h) throughout the experiment until the pre-defined endpoint or until the end-stage of the disease (defined below). All drug and vehicle treatments were coded, administered and analysed by a researcher blinded to the treatment groups.

### *Monitoring and behavioural assessments*

All mice were weighed and assessed in the morning (between 0900h – 1200h) 3 times per week as previously described (*18*) from the first day when they were switched to normal diet until the disease end-stage (defined as weight below 80% of initial weight on each of 3 consecutive days, or paralysis of both hindlimbs, or inability to right within 10 seconds from both sides). Motor behaviour was tested once weekly using grip strength, inverted grid and rotarod tests. Three training sessions for each of these tests were performed one week before the switch to standard diet.

For the neurological score assessment, mice were scored on a 4 point scale by an individual blinded to treatment group: 0, normal; 1, abnormal hindlimb splay, slightly slower gait, normal righting reflex; 2, hindlimb partially or completely collapsed, foot dragging along cage, slow righting reflex; 3, rigid paralysis in hindlimb or minimal movement, hindlimb is not being used for forward motion, slow righting reflex.

For the grip strength test, a digital force meter (Model 47200, Ugo Basile) was used to measure maximal muscle grip strength from all four limbs. Mice were held by the tail and placed in the centre of the grid connected to the force meter. The mice could use all four limbs to grip on the grid. The tail was pulled horizontally to the grid with a smooth steady manner until the mouse released the grid. The peak strength of the grip was measured in gram force. Each mouse was tested 3 times with at least 20

mins resting period between tests. The average of the highest two recordings was taken as the final result for analysis.

For the inverted grid test of muscle strength (also known as wirehang test), mice were placed on a customized metal grid (0.8 cm x 0.8 cm square grid, stainless steel), and gently flipped to be suspended upside down approximately 40 cm above a lightly padded clean cage. The time to fall was recorded up to a maximum 180 s. If a mouse did not perform the maximum time, three tests were performed with minimal interval of 20 mins resting period between tests, and the average of the longest two performances was taken as the final result for analysis.

For the rotarod test of motor coordination, balance and stamina, mice were placed on a rotarod apparatus (Model 7650, Ugo Basile) at a speed of 4 rpm with acceleration up to 40 rpm over 300 s (onset study) or 180 s (post-onset study). The time to fall was recorded, or the maximal time was recorded if mice were still on the rod without falling at the end of a session. Three tests were performed for each mouse with minimal interval of 20 mins, and the average of the longest two performance was taken as the final result for analysis.

***Perfusion and tissue collection***

Mice were deeply anesthetized using ketamine (100 mg/kg) and xylazine (10 mg/kg) and transcardially perfused with ~20 mL room temperature phosphate-buffered saline (0.01M PBS). Brains were removed under RNase free conditions and divided in half sagittal from the midline. The left hemisphere was quickly dissected to isolate the cortex, and this was immediately frozen on dry ice and stored at -80°C.

***Preparation of tissue lysates***

Tissues were thawed on ice and then sonicated in 5× v/w RIPA buffer with phosphatase and protease inhibitors (50 mM Tris, 150 mM NaCl, 1% NP-40, 5 mM EDTA, 0.5% sodium deoxycholate, 0.1% SDS, pH 8.0). Samples were centrifuged at 4°C, 100,000 *g* for 30 min and the supernatant taken as the RIPA-soluble fraction. The pellet was washed by sonication with RIPA buffer as above. This supernatant was discarded, and the pellet sonicated in 2× v/w urea buffer (7 M urea, 2 M thiourea, 4 % CHAPS, and 30 mM Tris, pH 8.5) and centrifuged at 22°C, 100,000 *g* for 30 min. This supernatant was taken as the RIPA-insoluble/urea-soluble fraction. Protein concentrations of the RIPA-soluble fractions were determined using the bicinchoninic

acid protein assay (Pierce) and volumes of urea-soluble protein used for immunoblotting were normalised to protein content of the matched RIPA sample.

***Immunoblotting***

Proteins were resolved by SDS-PAGE electrophoresis on BioRad polyacrylamide gels. For all immunoblots, 20 ug per sample were added to each well. Electrophoresis was carried out at 120 V for 1.5 hrs. Following electrophoresis, proteins were transferred to nitrocellulose membranes using the BioRad Transblot Turbo system. Membranes were incubated with 3% BSA for 1 hr, followed by exposure to the primary antibody. Primary antibodies included: rabbit anti-human/mouse TDP-43 1:5000 (Proteintech Cat# 10782-2-AP, RRID:AB_615042), mouse anti-human TDP-43 1:5000 (Clone 5104, (*19*)), mouse anti-phospho-TDP-43 (Ser409/410) (Cosmo Bio Co Cat# CAC-TIP-PTD-M01, RRID:AB_1961900), rabbit anti-EAAT2 1:1000 (Abcam Cat# ab178401), rabbit anti-GluA1 1:1000 (Abcam Cat# ab31232, RRID:AB_2113447), rabbit anti-GluA3 1:1000 (Abcam Cat# ab40845, RRID:AB_776310), and mouse anti-GAPDH 1:5000 (Proteintech Cat# 60004-1-Ig, RRID:AB_2107436), diluted in 0.1% BSA overnight at 4°C. Membranes were washed and incubated with LiCor 680/800 secondary antibodies (1:20,000) for 1 hr. Signals were detected using an Odyssey CLx and quantified with ImageStudio software.

***Statistical analyses***

All statistical analysis was performed using the statistical package Prism 7 (Graphpad). For normally distributed data, differences between means were assessed as appropriate, by one- or two- way ANOVA with or without repeated measures, followed by Bonferroni post hoc analysis. Simple effect tests were performed when group interactions were identified by ANOVA. The *p*-value, and F-statistic from ANOVA tests and associated degrees of freedom (between groups and within groups, respectively) are reported in parentheses. For neurological scoring, scores were square root transformed to produce a normal distribution. For survival curves, Kaplan-Meier survival tests were conducted. All data is presented as mean ± SEM. For all statistical tests, a $p$ value of $< 0.05$ was assumed to be significant.

## Results

We conducted two investigations in rNLS TDP-43 mice: a pre-onset study to determine the effects of riluzole when treatment began prior to motor symptoms, and; a post-onset study to investigate the more human-relevant scenario of riluzole treatment beginning after onset of motor deficits.

### *Riluzole does not delay onset or progression of motor deficits in rNLS mice*

The rNLS mice used in this study express the tetracycline transactivator protein (tTA) under the control of the human *NEFH* promotor, crossed with a *tetO*-hTDP-43ΔNLS line. This allows for doxycycline (dox)-suppressible expression of cytoplasmic hTDP-43 in neurons of the brain and spinal cord, resulting in a model of ALS amenable to pre-clinical therapeutic testing (*18, 20*).

First, to determine if riluzole treatment could delay the onset of ALS-like motor phenotypes, we conducted a series of assessments and behavioural tests in control and rNLS mice treated daily with vehicle or riluzole for 6 weeks, beginning at the initiation of hTDP-43ΔNLS expression by removal of dox. Since rNLS mice exhibit weight loss during disease progression (*18*), we assessed the ability of riluzole to modify weight changes over time. Mice were weighed three times weekly and an average of the three weights for each week was evaluated, expressed as a percentage of starting weight on day 1. A two-way ANOVA with repeated measures revealed a significant group by week interaction (Fig 1A; $F_{(15,95)}=23.74$, $p<0.001$), indicating differences in responses to treatment over time. Therefore, simple effects were assessed and as expected, significant differences were identified between vehicle-treated control and rNLS mice at weeks 5 and 6 off dox ($p<0.001$). However, no differences were observed between vehicle-treated or riluzole-treated rNLS mice, indicating that riluzole treatment had no effect on weight loss in rNLS mice.

To further assess changes to weight, we separated mice into four categories based on their maximum weight loss during the study (0-5, 5-10, 10-15 or >15% weight loss, Fig 1B). A Fisher pairwise comparison was performed ($p=0.78$) between riluzole- and vehicle-treated rNLS mice. 100% of vehicle-treated rNLS mice showed a weight loss of >15% over the 6-week treatment period, whereas only 50% of riluzole treated mice

showed a weight loss of >15%, suggesting a trend towards lower maximum weight loss in riluzole-treated rNLS mice.

rNLS mice develop neurological deficits that can be assessed on a 4-point scale. We found no significant differences over time in these neurological scores of vehicle- or riluzole-treated rNLS mice (Fig 1C). No control mice showed any signs of neurological deficits, as expected.

To assess if riluzole can improve motor deficits observed in rNLS mice, we performed comprehensive behavioural testing. Grip strength was measured to determine changes in neuromuscular strength, coordination and functional capacity. There was a significant interaction between group and week (Fig 1D; $F_{(18,114)}=20.6$ $p<0.001$), indicating differential change over time in test performance. As expected, significant differences of vehicle-treated control vs vehicle-treated rNLS mice occurred from weeks 3 to 6 ($p<0.001$), confirming a significant muscle weakening as a result of hTDP-43ΔNLS expression in rNLS mice. There was no difference between vehicle- or riluzole-treated control mice at any week, demonstrating no effect of riluzole in wildtype animals. However, there was also no difference between vehicle- or riluzole-treated rNLS mice at any week, indicating no effect of the treatment on grip strength in rNLS mice, despite disease-associated decline in this task over time in these animals.

To further test neuromuscular balance and strength, we performed the inverted grid test on vehicle- or riluzole-treated control and rNLS mice. A significant interaction effect of group by week was found (Fig 1E; $F_{(18,114)}=6.18$ $p<0.001$), indicating differential change between groups over time in test performance. Vehicle-treated rNLS mice exhibited significantly decreased time to fall from the inverted grid as compared to vehicle-treated control mice from weeks 2 to 6 ($p<0.001$), confirming the results observed in previous studies (*18*). However, no differences were observed between vehicle- or riluzole-treated rNLS mice at any time point, indicating no effect of riluzole on the observed muscle weakness in rNLS mice.

As an additional test of motor impairment, we analysed the time spent on an accelerating rotarod. A two-way ANOVA with repeated measures revealed a significant interaction of group by week (Fig 1F; $F_{(18,114)}=10.23$ $p<0.001$), indicating differential change over time in rotarod performance. Similar to the grip strength and inverted grid test results, a significant difference occurred between vehicle-treated

control mice and vehicle-treated rNLS mice from weeks 2 to 6 ($p<0.001$), confirming the progressive motor deficits of the rNLS mouse model reported previously (*18*). However, there were no significant differences between vehicle- or riluzole-treated rNLS mice in rotarod performance, again indicating no effect of riluzole treatment on motor function.

Overall, we observed no effect of riluzole on any behavioural test when mice were treated from day 0 of hTDP-43ΔNLS expression until 6 weeks after removal of dox, by which time all rNLS mice were severely impaired in motor functions.

### *Riluzole does not alter soluble or insoluble TDP-43 protein levels in rNLS mice*

Accumulation of aggregated and phosphorylated TDP-43 is the main pathological hallmark of ALS (*16*), and thus amelioration of TDP-43 accumulation is likely to be a key marker of therapeutic efficacy in disease. Therefore, we next assessed TDP-43 levels in the rNLS mice following riluzole treatment. To determine if riluzole altered the levels of soluble TDP-43 (primarily indicating non-aggregated functional protein), cortex samples from vehicle- or riluzole-treated control and rNLS mice were separated into RIPA-soluble and urea-soluble fractions (Fig 2A). Previous studies indicate robust detection of both soluble and insoluble TDP-43 in rNLS mice at 6 weeks after removal of Dox (*18*), and therefore this time point was chosen to assess the effects of riluzole. As expected, one-way ANOVA revealed significant differences in RIPA-soluble hTDP-43ΔNLS (indicating levels of the human transgene, Fig 2B; $F_{(3,12)}=111$ $p<0.001$) and h+mTDP-43 (detecting both endogenous and human TDP-43, Fig 2C; $F_{(3,12)}=26.72$ $p<0.001$) between all four treatment groups. Post-hoc analysis revealed that levels of RIPA-soluble TDP-43 did not differ in control mice regardless of riluzole treatment, although rNLS mice had significantly higher levels of RIPA-soluble TDP-43 than control mice as expected. Furthermore, there were no significant differences between the levels of RIPA-soluble hTDP-43ΔNLS or h+mTDP-43 in the cortex of vehicle- or riluzole-treated rNLS mice. Together these findings indicate that riluzole treatment had no effect on soluble TDP-43 levels in either control or rNLS animals.

We next assessed levels of TDP-43 in the RIPA-insoluble/urea-soluble protein fraction, which contains aggregated/pathological proteins. A one-way ANOVA

revealed significantly different levels of both RIPA-insoluble hTDP-43ΔNLS (Fig 2D; $F_{(3,12)}=24.59$ $p<0.001$) and h+mTDP-43 (Fig 2E; $F_{(3,12)}=8.13$ $p<0.05$) between groups. Post-hoc analysis revealed a significant difference in urea-soluble hTDP-43ΔNLS and h+mTDP-43 levels in both vehicle- or riluzole-treated rNLS mice compared to vehicle-treated control mice. Notably, there were no statistically significant differences in urea-soluble hTDP-43ΔNLS or h+mTDP-43 levels between vehicle- or riluzole-treated rNLS mice, indicating that riluzole had no effect on accumulation of aggregated TDP-43 in disease. Likewise, levels of phosphorylated TDP-43 (pS409/410) in the urea-soluble fraction were not altered between vehicle- or riluzole-treated rNLS mice (Fig 2F). Combined, these results indicate that riluzole treatment does not alter TDP-43 levels, phosphorylation or solubility in rNLS mice.

***GluA3, but not GluA1, glutamate receptor subunit levels are decreased in rNLS mice but are unaltered by riluzole***

In the mouse brain, TDP-43 binds specifically to mRNAs of the AMPA receptor subunits *Gria2* (encoding GluA2), *Gria3* (GluA3) and *Gria4* (GluA4), but not *Gria1* (GluA1) (*21, 22*). Indeed, TDP-43 has been shown to bind to the intronic pre-mRNA of *Gria3*, and knockdown of TDP-43 in mouse brain causes both splicing changes and a decrease in levels of *Gria3* mRNA (*23, 24*). Increased surface levels of GluA1 are also observed in neurons expressing ALS-linked TDP-43$^{A315T}$ *in vitro* (*25*). Combined, these studies indicate that multiple mechanisms likely relate altered TDP-43 function to specific changes in AMPA receptor levels, and these changes may contribute to excitotoxic neuron loss in ALS. Likewise, previous studies have indicated that riluzole can mediate the activity of AMPA receptors *in vitro* (*26*). Together, these studies indicate that both TDP-43 function and riluzole affect levels and function of the glutamatergic neurotransmission machinery.

To determine if riluzole can modulate AMPA receptor levels in rNLS mice, we immunoblotted for the GluA1 and GluA3 receptors in vehicle- or riluzole-treated control and rNLS mice (Fig 3A). A one-way ANOVA revealed no overall changes in GluA1 levels (Fig 3B; $p=0.72$) between each of the four groups. However, GluA3 levels were significantly decreased in vehicle-treated rNLS mice compared to vehicle-treated control mice (Fig 3C; $p<0.0001$), suggesting specific loss of glutamate receptor

subunits during disease. Despite the proposed mechanism of action of riluzole being in part due to non-competitive inhibition of AMPA receptors (*27*) in disease, there were no differences in GluA3 levels between vehicle- or riluzole-treated rNLS mice, indicating an inability of riluzole to rescue the disease-associated GluA3 deficiencies.

In addition to AMPA receptors, riluzole has been shown to upregulate GLT-1 (EAAT2) expression in astrocytes *in vitro* (*28*). We therefore assessed EAAT2 levels in vehicle- or riluzole-treated control and rNLS mice. A one-way ANOVA revealed no overall changes to EAAT2 in rNLS mice compared to control mice (Fig 3E; $p$=0.17). Likewise, riluzole treatment did not significantly alter EAAT2 levels. Collectively, our results demonstrate that selective alteration in levels of glutamate receptor subunits occur in the rNLS mice, but that riluzole treatment does not affect levels of specific AMPA receptor subunits or EAAT2 in mouse cortex.

***Riluzole does not alter developed motor deficits or extend lifespan in rNLS mice***

Recent epidemiological analyses of people with ALS treated with riluzole have indicated that the potential disease-delaying effects of the drug are likely to occur only in the earliest and latest stages of disease (*3, 29*). Since we showed above that riluzole had no effect in the earliest stages of disease in the rNLS mice, we next performed an additional study in which treatment began at 4 weeks post-disease induction, when motor deficits and neurological changes had already developed in the rNLS mice (*18*), and studied the mice until the humane disease end-stage. We assessed mouse weights both prior to and during vehicle or riluzole treatment. Assessing changes in mean mouse weights with two-way ANOVA with repeated measures revealed a significant group by week interaction (Fig 4A; $F_{(12,112)}$=57.25, $p$<0.001), indicating a differential change in weight over time, and so simple effects were evaluated. Significant differences were detected between vehicle-treated control and rNLS mice at 4, 6 and 8 weeks after removal of dox ($p$<0.001), as expected. Furthermore, no differences occurred between vehicle- or riluzole-treated rNLS mice both prior to or during riluzole treatment, indicating no treatment effect of riluzole in rNLS mice once weight loss was established. A Fisher exact test to categorically assess binned maximum weight loss revealed no differences between vehicle- or riluzole- treated

rNLS mice (Fig 4B; $p$=1), again indicating that riluzole treatment had no effect on disease-associated weight loss.

Neurological deficits were also assessed prior to and during treatment. Vehicle- or riluzole-treated control mice showed no signs of neurological deficits on the 4-point scale (Fig 4C). Neurological deficits were apparent with a mean score above 1 in rNLS mice by approximately day 18. However, there were no significant differences over time between vehicle- or riluzole-treated rNLS mice (Fig 4C), indicating that riluzole treatment had no effect on development or progression of neurological deficits in the rNLS mice.

We also tested motor behaviour to determine if administration of riluzole beginning after onset of motor deficits could alter disease phenotypes. Grip strength analysis was performed both prior to and during treatment with vehicle or riluzole. A two-way ANOVA with repeated measures revealed a significant interaction of group by week (Fig 4D; $F_{(12,80)}=24.34$ $p<0.001$), indicating differential changes to group performance over time. A progressive decline in grip strength was apparent in vehicle-treated rNLS mice, with significant decline in grip strength force in rNLS mice apparent at 4, 6 and 8 weeks ($p<0.001$). However, progression of muscle weakness was not altered by post-onset treatment with riluzole, since no differences were apparent between vehicle- or riluzole-treated rNLS mice at any time point.

Similar results were observed in the inverted grid test, where a two-way ANOVA with repeated measures revealed a significant interaction of group by week (Fig 4E; $F_{(12,80)}=27.16$ $p<0.001$). Despite significant differences between vehicle-treated control and rNLS mice at 4, 6, and 8 weeks ($p<0.001$), no changes occurred between vehicle- or riluzole-treated rNLS mice in any week, indicating that riluzole was unable to improve muscle strength in these animals.

In addition, a two-way ANOVA with repeated measures revealed a significant interaction of group by week in the rotarod test (Fig 4F; $F_{(12,80)}=7.134$ $p<0.001$), indicating differential changes over time, and thus post-hoc simple effects were analysed. There were significant differences in rotarod performance between vehicle-treated control and rNLS mice at 4, 6, and 8 weeks ($p<0.001$), as expected. However, there was no difference in performance of vehicle- or riluzole-treated rNLS mice at any time point. Overall, these results show that administration of riluzole starting post-

disease onset, once motor deficits and neurodegeneration are already established, does not alter the behavioural phenotype observed in rNLS mice.

Finally, we aimed to determine if riluzole could extend lifespan, since a shortened period of survival is characteristic of rNLS mice expressing hTDP-43ΔNLS (*18*). Age, sex and litter-matched rNLS mice were treated with vehicle or riluzole from 4 weeks after induction of hTDP-43ΔNLS expression, and lifespan was measured from day off dox until humane disease end-stage (Fig. 4G). A Kaplan-Meir survival curve revealed no differences between riluzole- or vehicle-treated animals ($\chi^2$=0.01, d.f=1 and *p*=0.91) with a median survival of 76 days for vehicle-treated and 80 days for riluzole-treated rNLS mice. Combined, these results indicate that riluzole had no effect on motor impairment or lifespan in rNLS mice when treatment began following disease onset.

## Discussion

ALS is a progressive fatal neurodegenerative disease with limited therapeutic options. First demonstrated to provide modest survival extension to people with ALS over two decades ago, riluzole remains the most widely prescribed treatment for ALS. However, the mechanisms of action of this drug remain poorly defined and whether riluzole can modify underlying disease-related pathological changes is unclear. In this study, we sought to investigate the effects of riluzole in the well-characterised rNLS TDP-43 mouse model, which develops a progressive ALS-like disease driven by the accumulation of cytoplasmic TDP-43 in neurons of the brain and spinal cord. We showed that riluzole administration does not alter disease onset, progression or survival of rNLS TDP-43 mice. Likewise, riluzole did not alter levels of soluble, insoluble or phosphorylated TDP-43. Interestingly, we found that levels of the AMPA receptor subunit GluA3 are significantly lower in the cortex of rNLS TDP-43 mice, which parallels changes to glutamatergic signalling observed in people with ALS. However, riluzole treatment was unable to correct this disease-related change in glutamate receptors, despite previous studies suggesting that riluzole may modulate glutamatergic excitotoxicity. Overall, our study further substantiates the limited benefit of riluzole in modifying ALS-like pathology and disease phenotypes in mice.

TDP-43 aggregation is a major neuropathological feature of ALS, and targeting of TDP-43 dysfunction will likely be important for development of effective disease-modifying treatments. Our study is the first to indicate that riluzole administration does not alter total levels of TDP-43, nor does riluzole affect accumulation of insoluble and phosphorylated TDP-43. Recent studies have suggested that riluzole may exert its actions through a direct link on TDP-43 self-interaction, without change to total TDP-43 levels in neuroblastoma cells *in vitro* (*30*). Furthermore, it has been hypothesised that expression of a truncated protein kinase, CK1δ, leads to phosphorylation, mislocalisation and aggregation of TDP-43 (*31*), and that riluzole is may inhibit this process (*10*). However, in contrast to these results, we observed no alteration of TDP-43 phosphorylation nor decreases to insoluble TDP-43 with riluzole treatment, indicating that riluzole may not exert these effects *in vivo.*

AMPA receptors are tetrameric assemblies of four subunits designated GluA1–GluA4, which modulate fast excitatory neurotransmission in the brain. Our finding of a decrease in protein levels of GluA3 in the cortex of rNLS mice at 6 weeks after dox suggests that specific changes in glutamatergic neurotransmission system occur in this model, with potential implications for understanding mechanisms of ALS pathogenesis. Motor neurons are intrinsically vulnerable to altered glutamatergic signalling due to their relative high density of AMPA receptor currents (*32*). However, both hyperexcitability and hypoexcitability have been implicated in the pathogenesis of ALS, and a plethora of studies indicate that this phenotype is a complex and evolving phenomenon (*33*). The role that TDP-43 plays in this alteration in excitability is unclear, however it may be affecting the system by both direct and indirect mechanisms. Previous studies have shown that TDP-43 binds directly to mRNA of *Gria3* (the gene encoding GluA3), to regulate both splicing and total levels of *Gria3*, and TDP-43 knockdown results in lowered *Gria3* levels (*21-24*). In the TDP-43 rNLS mice, there is a decrease in levels of normal nuclear mouse TDP-43, likely due to TDP-43 auto-regulation upon increased levels of cytoplasmic human TDP-43 (*18, 34*), suggesting that the specific decrease in GluA3 protein levels that we detected may be due to a loss of function of nuclear TDP-43 in this model. This finding suggests that despite the dramatic accumulation of aggregation-prone cytoplasmic TDP-43 in neurons in these mice (*18*), at least some of the ALS-like molecular features that occur may be due to loss of normal TDP-43. It may also be plausible that a down-regulation of GluR3 may be a compensatory mechanism due to increased glutamatergic signalling that may ultimately lead to a hypoexcitability phenotype, which has been attributed to the demise of spinal motor neurons (*35*). Together, these findings suggest multiple mechanisms related to alterations in glutamatergic neurotransmission may be involved in ALS pathogenesis, and how alterations in levels of different glutamate receptors change over time in disease remains to be addressed. Further investigation of how alterations in levels and localisation of AMPA receptor subunits affect disease is warranted in TDP-43 models such as the rNLS mice, and in ALS.

It may be also worthwhile to consider other potential disease-relevant effects of riluzole to understand the effects of this drug and to identify worthy options for future focus of therapeutic development. Previously, riluzole has been shown to enhance

the activity of several glutamate transporters, including the primarily astrocytic EAAT2 (also known as GLT-1) (*36*). Likewise, in astrocyte cell culture riluzole treatment increased both EAAT2 levels and activity (*37*). Treatment of rats with riluzole reversed ageing-related loss of EAAT2 in the hippocampus (*38*), and likewise in a transgenic mouse model of tau-associated neurodegeneration there is a decrease in EAAT2 in the hippocampus which is ameliorated by riluzole (*39*). Early studies indicated that decreased glutamate transport and suppressed levels of EAAT2 in astrocytes of the brain and spinal cord are features of disease in people with ALS (*40, 41*), and loss of EAAT2 has also been shown in tissues of people who died with frontotemporal lobar degeneration with TDP-43 pathology (*42*). Since EAAT2 is involved in clearance of glutamate from synapses, loss of this protein from astrocytes may contribute to excitotoxicity seen in ALS. In our study, we saw no change in EAAT2 protein levels at 6 weeks after removal of dox in the rNLS TDP-43 mice. Likewise, we did not see an effect of riluzole on EAAT2 levels, although an effect may have been masked by the lack of a disease-related decline in total EAAT2 levels in the cortex of the rNLS TDP-43 mice. Astrogliosis is a feature of disease in the rNLS TDP-43, similar to human ALS, and begins in the early stages of disease progression (*18*). How astrocytic changes contribute to progression of TDP-43-related disease also remains unclear, however our findings suggest that EAAT2 changes are not necessarily concomitant with alterations in astrocytic activation. Further studies are required to investigate whether the rNLS TDP-43 mice show alterations in levels of these and other proteins involved in glutamatergic neurotransmission and glutamate scavenging at earlier and late stages of disease, which may reveal specificity in the timing of these changes related to disease onset and progression.

We showed previously in the rNLS TDP-43 mice that by returning mice to dox after neurodegeneration had begun and when mice had a severe motor phenotype, that functional recovery is possible, raising hope that stabilisation and even improvement of disease signs is potentially possible in people with ALS even after disease has progressed (*18*). For treatment of ALS, it is likely that methods that modulate key aspects of disease, such as decreasing TDP-43 aggregation or causing specific changes in function and excitability of motor neurons, will need to be identified that

may not individually ameliorate all aspects of disease but in combination may prove highly effective. This is also important to consider in the case of riluzole, since it has been shown that although riluzole alone had no effect in SOD1$^{G93A}$ mice, when combined with elacridar, a drug which inhibits transporters including P-glycoprotein that control drug efflux from the central nervous system, motor function was improved and survival was significantly extended (*43*). P-glycoprotein is up-regulated in ALS at least in part in response to astrocytic release of glutamate, and this up-regulation may decrease penetration of riluzole into the central nervous system (*44*). These findings suggest that combination therapy of other drugs with riluzole may prove to be effective, and studies of this approach in valid TDP-43 mouse models of disease are needed.

In summary, we have identified specific alterations in levels of some glutamatergic neurotransmission-related proteins in the rNLS TDP-43 mice, however riluzole, largely thought to act through this pathway, is unable to alter the ALS-like disease course or extend survival in this model. This is concordant with previous mouse studies that saw no effect of riluzole in SOD1$^{G93A}$ mice (*14*), or TDP-43$^{A315T}$ or FUS transgenic mouse models of ALS (*15*). These studies highlight the importance of tailoring the use of animal models to the experimental question being addressed, to ensure translatability of findings; although models such as the rNLS TDP-43 mice are useful to study molecular mechanisms of ALS they may not necessarily recapitulate every aspect of human disease. In future studies, this model will most likely be most powerful for analysis of therapeutics designed to directly target the dysfunctional molecular pathways related to aggregation and cytoplasmic accumulation of TDP-43. Indeed, renewed focus on understanding these and other core molecular signatures of ALS and design of new strategies to modulate the upstream causes of disease offer potential for more effective treatments for this devastating condition.

***Acknowledgements***

We thank Prof. Virginia Lee (University of Pennsylvania) for the TDP-43 antibody (clone 5104).

***Conflict of interest***

The authors declare no conflict of interest.

***Funding***

This work was supported by an Australian Government Research Training Program Scholarship to BAB, the MND Research Institute of Australia (PhD top-up scholarship to BAB and Cure for MND Research Grant 1651 to AKW), the Australian National Health and Medical Research Council (Project Grant 1124005 and RD Wright Career Development Fellowship 1140386 to AKW), donations made to the Macquarie University Centre for Motor Neuron Disease Research, the Ross Maclean Fellowship, and the Brazil Family Program for Neurology.

***Author contributions***

ALW, SL and AKW wrote the paper. ALW, SL, PM, PDG, BAB, KRJ, HG, RSG, TJH, WRR, OW and AKW performed experiments. ALW, SL, SSK and AKW analysed data. RSC, JDA, AL, BS, CAB and MM provided reagents and guidance. AKW supervised the study.

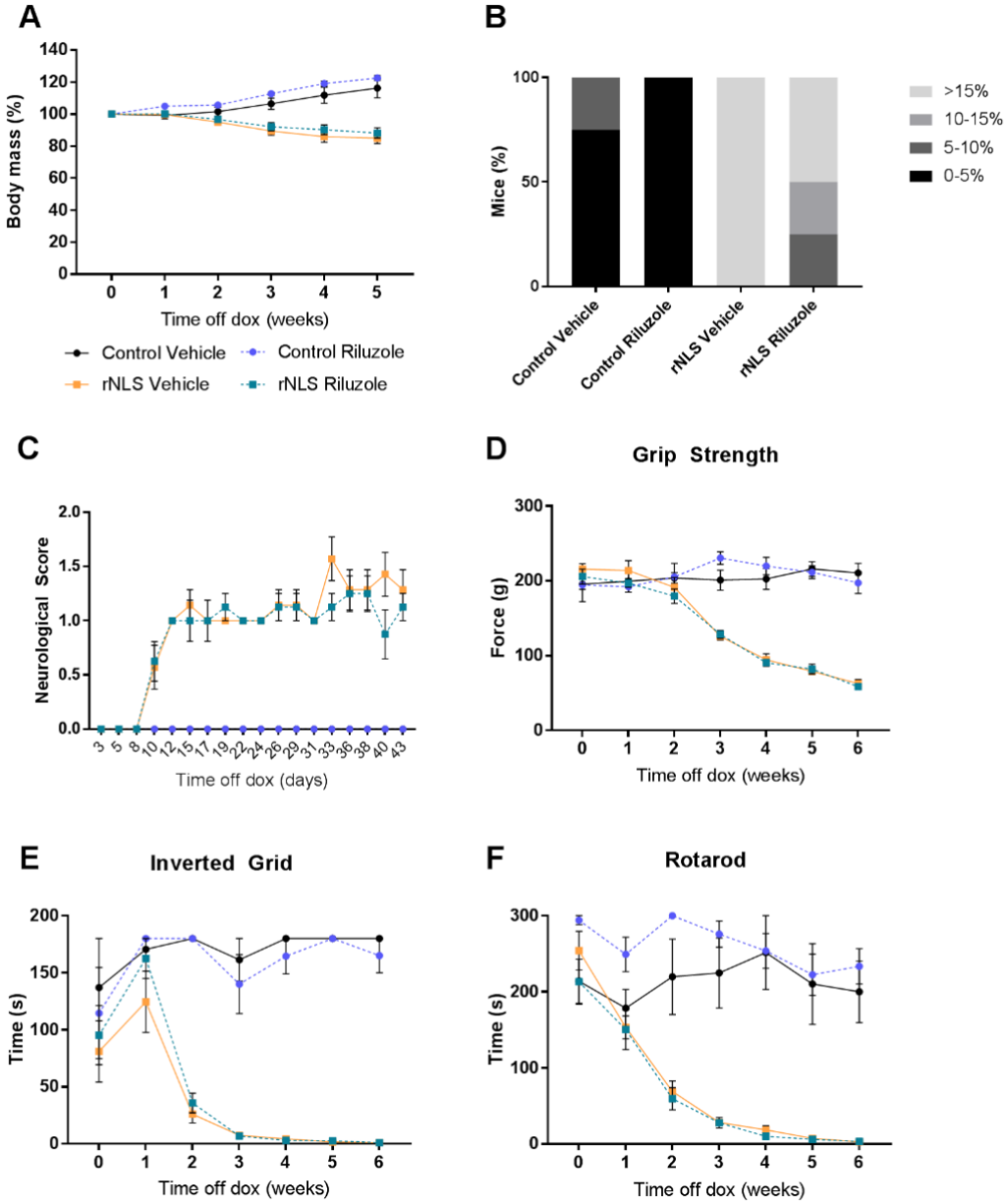


***Figure 1. Riluzole treatment beginning at time off dox does not alter body mass change or motor behaviour in control or TDP-43 rNLS mice.*** **A** Percentage of the pre-disease (day 0) body mass showed significant weight loss over time in rNLS mice, which was not altered by riluzole. **B** Total percentage of mice treated that had maximum body weight loss of 0-5, 5-10, 10-15 or >15% indicated greater weight loss in rNLS mice compared to controls, with trend towards preservation of weight in riluzole-treated rNLS mice. **C** No significant differences in neurological scores occurred between vehicle- or riluzole-treated rNLS mice. Behavioural assessment of motor function was performed in vehicle- or riluzole-treated control and rNLS mice from day of dox removal, for 6 weeks. No significant differences between vehicle- and riluzole-treated mice were seen in **D** grip strength, **E** inverted grid test, or **F** rotarod tests. Corresponding graph colours as per **A**, i.e. control vehicle = black solid line, control riluzole = blue dashed line, rNLS vehicle = orange solid line, rNLS riluzole = green dashed line. *n*=4/control group, *n*=7 rNLS vehicle and *n*=8 rNLS riluzole.

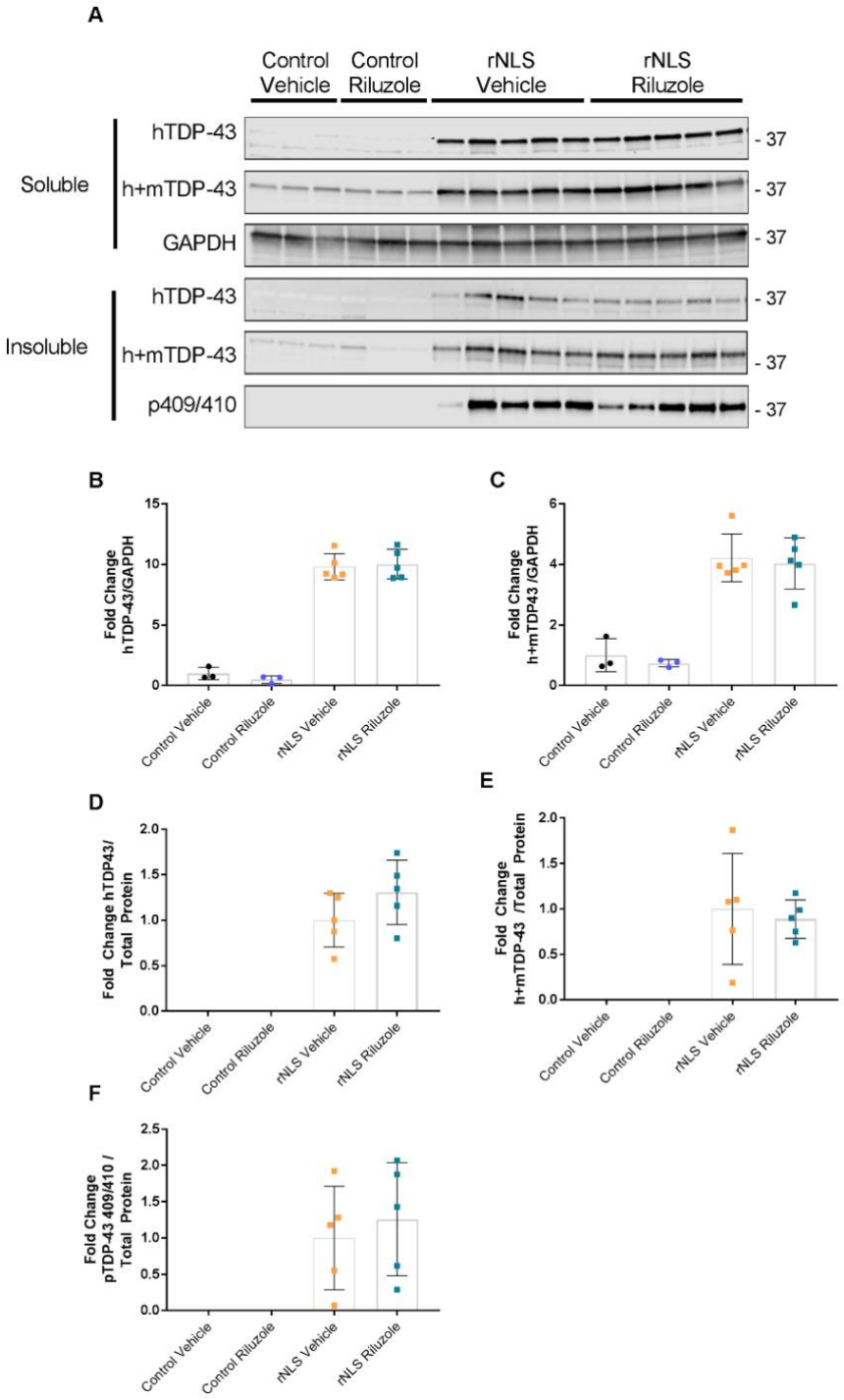


***Figure 2. Riluzole treatment does not alter RIPA-soluble and -insoluble total and phosphorylated TDP-43 levels in control and TDP-43 rNLS mice.*** **A** Representative immunoblots of RIPA-soluble and urea-soluble cortical brain lysates from vehicle- or riluzole-treated control and rNLS mice for human-specific (h)TDP-43, human- and mouse-specific (h+m)TDP-43 and phosphorylated (p409/410) TDP-43. Quantification of **B** RIPA-soluble hTDP-43ΔNLS, **C** RIPA-soluble h+mTDP-43, **D** urea-soluble hTDP-43ΔNLS, **E** urea-soluble h+mTDP-43, and **F** p409/410 TDP-43 revealed significantly higher levels in vehicle-treated rNLS mice compared to vehicle- or riluzole-treated control mice, but these were not different to riluzole-treated rNLS mice. *n*=3/control group and *n*=5/rNLS group.

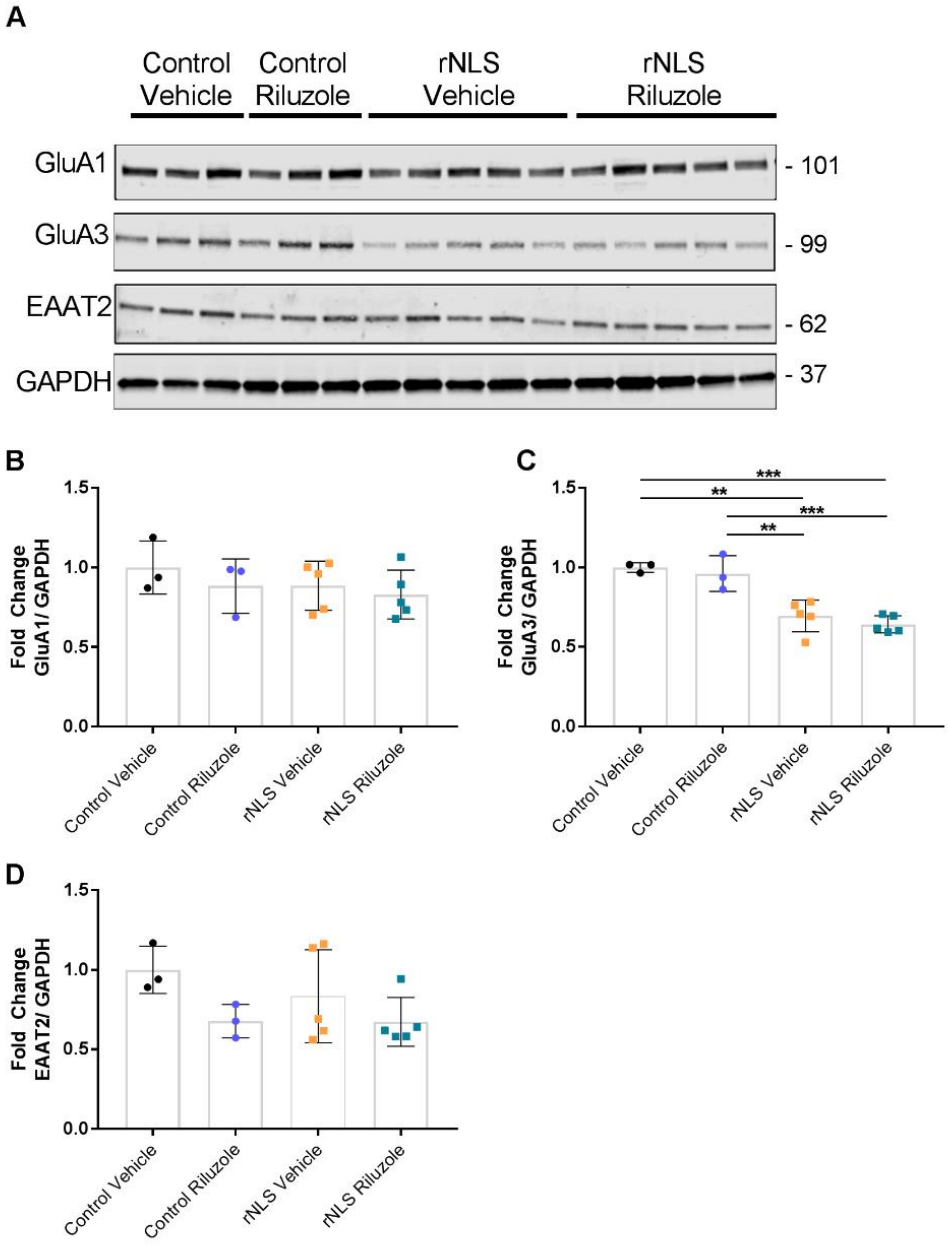


***Figure 3. Levels of AMPA receptor subunit GluA3, but not GluA1 or the glutamate-transporter EAAT2, are decreased in rNLS TDP-43 mice but are not altered by riluzole treatment***. **A** Representative immunoblots of RIPA-soluble cortical brain lysates from vehicle- or riluzole-treated control and rNLS mice for GluA1, GluA3 and EEAT2. **B** Quantification revealed no significant differences of GluA1 between all four treatment groups. **C** Quantification revealed significant lower levels of GluA3 in rNLS mice compared to control, with no effect of riluzole treatment. **D** No significant changes were observed in EAAT2 levels between groups. *n*=3/control group and *n*=5/rNLS group. **=$p<0.01$, ***=$p<0.001$.

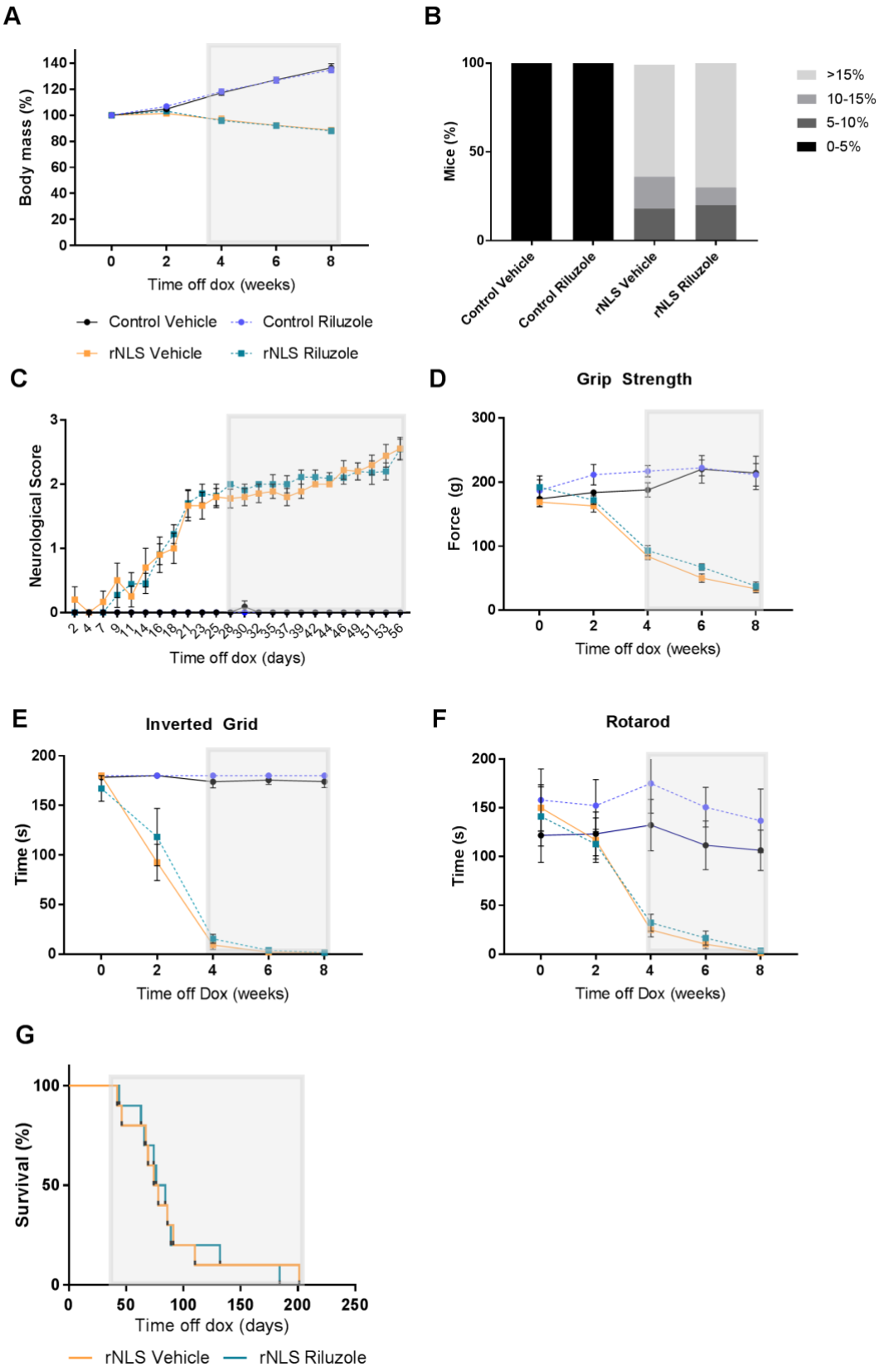


***Figure 4. Riluzole treatment beginning after disease onset does not alter body mass loss, motor behaviour or survival in TDP-43 rNLS mice.*** **A** Percentage of the pre-disease

(day 0) body mass showed significant weight loss over time in rNLS mice, which was not altered by riluzole (*n*=8/group). **B** Total percentage of mice treated that had maximum body weight loss of 0-5, 5-10, 10-15 or >15% indicated greater weight loss in rNLS mice compared to control (*n*=8/group). **C** No significant differences in neurological scores occurred between vehicle- or riluzole-treated rNLS mice (*n*=11 for control vehicle, control riluzole and rNLS riluzole and *n*=10 for rNLS vehicle). Behavioural assessment of motor function testing was analysed in vehicle- and riluzole-treated control and rNLS mice from day of dox removal, for 8 weeks, after which some rNLS mice began to reach humane disease end-stage. No significant differences between vehicle- and riluzole-treated mice were seen in **D** grip strength, **E** inverted grid test, or **F** rotarod tests (*n*=6/group). **G** Kaplan-Meier analysis of survival in vehicle- or riluzole-treated rNLS mice revealed no significant effect of riluzole treatment on lifespan (*n*=10/group). Corresponding graph colours as per **A**, i.e. control vehicle = black solid line, control riluzole = blue dashed line, rNLS vehicle = orange solid line, rNLS riluzole = green dashed line. Grey box indicates period during which mice were treated with vehicle or riluzole (daily from 4 weeks after removal of dox).

## References


1. W. Robberecht, T. Philips, The changing scene of amyotrophic lateral sclerosis. *Nat Rev Neurosci* **14**, 248-264 (2013).
2. L. Lacomblez, G. Bensimon, P. N. Leigh, P. Guillet, V. Meininger, Dose-ranging study of riluzole in amyotrophic lateral sclerosis. Amyotrophic Lateral Sclerosis/Riluzole Study Group II. *Lancet* **347**, 1425-1431 (1996).
3. T. Fang *et al.*, Stage at which riluzole treatment prolongs survival in patients with amyotrophic lateral sclerosis: a retrospective analysis of data from a dose-ranging study. *Lancet Neurol* **17**, 416-422 (2018).
4. R. G. Miller, J. D. Mitchell, D. H. Moore, Riluzole for amyotrophic lateral sclerosis (ALS)/motor neuron disease (MND). *Cochrane Database Syst Rev*, CD001447 (2012).
5. M. C. Bellingham, A review of the neural mechanisms of action and clinical efficiency of riluzole in treating amyotrophic lateral sclerosis: what have we learned in the last decade? *CNS Neurosci Ther* **17**, 4-31 (2011).
6. J. D. Rothstein *et al.*, Abnormal excitatory amino acid metabolism in amyotrophic lateral sclerosis. *Ann Neurol* **28**, 18-25 (1990).
7. M. L. Martinez-Silva *et al.*, Hypoexcitability precedes denervation in the large fast-contracting motor units in two unrelated mouse models of ALS. *Elife* **7**, (2018).
8. T. Jiang *et al.*, Amyotrophic lateral sclerosis mutant TDP-43 may cause synaptic dysfunction through altered dendritic spine function. *Dis Model Mech* **12**, (2019).
9. C. Klemann, J. E. Visser, L. Van Den Bosch, G. J. M. Martens, G. Poelmans, Integrated molecular landscape of amyotrophic lateral sclerosis provides insights into disease etiology. *Brain Pathol* **28**, 203-211 (2018).
10. M. Bissaro *et al.*, Targeting Protein Kinase CK1delta with Riluzole: Could It Be One of the Possible Missing Bricks to Interpret Its Effect in the Treatment of ALS from a Molecular Point of View? *ChemMedChem* **13**, 2601-2605 (2018).
11. M. P. Shaw *et al.*, Stable transgenic C9orf72 zebrafish model key aspects of the ALS/FTD phenotype and reveal novel pathological features. *Acta neuropathologica communications* **6**, 125 (2018).

12. M. E. Gurney *et al.*, Benefit of vitamin E, riluzole, and gabapentin in a transgenic model of familial amyotrophic lateral sclerosis. *Ann Neurol* **39**, 147-157 (1996).
13. M. E. Gurney, T. J. Fleck, C. S. Himes, E. D. Hall, Riluzole preserves motor function in a transgenic model of familial amyotrophic lateral sclerosis. *Neurology* **50**, 62-66 (1998).
14. S. Scott *et al.*, Design, power, and interpretation of studies in the standard murine model of ALS. *Amyotrophic lateral sclerosis : official publication of the World Federation of Neurology Research Group on Motor Neuron Diseases* **9**, 4-15 (2008).
15. M. C. Hogg, L. Halang, I. Woods, K. S. Coughlan, J. H. M. Prehn, Riluzole does not improve lifespan or motor function in three ALS mouse models. *Amyotroph Lateral Scler Frontotemporal Degener* **19**, 438-445 (2018).
16. M. Neumann *et al.*, Ubiquitinated TDP-43 in frontotemporal lobar degeneration and amyotrophic lateral sclerosis. *Science (New York, N.Y.)* **314**, 130-133 (2006).
17. S. C. Ling, M. Polymenidou, D. W. Cleveland, Converging mechanisms in ALS and FTD: disrupted RNA and protein homeostasis. *Neuron* **79**, 416-438 (2013).
18. A. K. Walker *et al.*, Functional recovery in new mouse models of ALS/FTLD after clearance of pathological cytoplasmic TDP-43. *Acta Neuropathol* **130**, 643-660 (2015).
19. L. K. Kwong *et al.*, Novel monoclonal antibodies to normal and pathologically altered human TDP-43 proteins. *Acta Neuropathol Commun* **2**, 33-33 (2014).
20. K. J. Spiller *et al.*, Reduction of matrix metalloproteinase 9 (MMP-9) protects motor neurons from TDP-43-triggered death in rNLS8 mice. *Neurobiol Dis* **124**, 133-140 (2019).
21. C. F. Sephton *et al.*, Identification of neuronal RNA targets of TDP-43-containing ribonucleoprotein complexes. *J Biol Chem* **286**, 1204-1215 (2011).
22. R. K. Narayanan *et al.*, Identification of RNA bound to the TDP-43 ribonucleoprotein complex in the adult mouse brain. *Amyotroph Lateral Scler Frontotemporal Degener* **14**, 252-260 (2013).
23. C. Lagier-Tourenne *et al.*, Divergent roles of ALS-linked proteins FUS/TLS and TDP-43 intersect in processing long pre-mRNAs. *Nat Neurosci* **15**, 1488-1497 (2012).

24. M. Polymenidou *et al.*, Long pre-mRNA depletion and RNA missplicing contribute to neuronal vulnerability from loss of TDP-43. *Nat Neurosci* **14**, 459-468 (2011).
25. T. Jiang *et al.*, Amyotrophic lateral sclerosis mutant TDP-43 may cause synaptic dysfunction through altered dendritic spine function. *Disease Models & Mechanisms* **12**, dmm038109 (2019).
26. J. Du *et al.*, The anticonvulsants lamotrigine, riluzole, and valproate differentially regulate AMPA receptor membrane localization: relationship to clinical effects in mood disorders. *Neuropsychopharmacology : official publication of the American College of Neuropsychopharmacology* **32**, 793-802 (2007).
27. F. Albo, M. Pieri, C. Zona, Modulation of AMPA receptors in spinal motor neurons by the neuroprotective agent riluzole. *Journal of Neuroscience Research* **78**, 200-207 (2004).
28. M. Carbone, S. Duty, M. Rattray, Riluzole elevates GLT-1 activity and levels in striatal astrocytes. *Neurochem Int* **60**, 31-38 (2012).
29. A. D. de Jongh, R. P. A. van Eijk, L. H. van den Berg, Evidence for a multimodal effect of riluzole in patients with ALS? *J Neurol Neurosurg Psychiatry*, (2019).
30. M. Oberstadt *et al.*, TDP-43 self-interaction is modulated by redox-active compounds Auranofin, Chelerythrine and Riluzole. *Scientific Reports* **8**, 2248 (2018).
31. T. Nonaka *et al.*, Phosphorylation of TAR DNA-binding Protein of 43 kDa (TDP-43) by Truncated Casein Kinase 1δ Triggers Mislocalization and Accumulation of TDP-43. *Journal of Biological Chemistry* **291**, 5473-5483 (2016).
32. L. Van Den Bosch, W. Vandenberghe, H. Klaassen, E. Van Houtte, W. Robberecht, Ca(2+)-permeable AMPA receptors and selective vulnerability of motor neurons. *J Neurol Sci* **180**, 29-34 (2000).
33. R. Clark, C. Blizzard, T. Dickson, Inhibitory dysfunction in amyotrophic lateral sclerosis: future therapeutic opportunities. *Neurodegener Dis Manag* **5**, 511-525 (2015).
34. L. M. Igaz *et al.*, Dysregulation of the ALS-associated gene TDP-43 leads to neuronal death and degeneration in mice. *J Clin Invest* **121**, 726-738 (2011).

35. N. Delestrée *et al.*, Adult spinal motoneurones are not hyperexcitable in a mouse model of inherited amyotrophic lateral sclerosis. *The Journal of Physiology* **592**, 1687-1703 (2014).
36. E. Fumagalli, M. Funicello, T. Rauen, M. Gobbi, T. Mennini, Riluzole enhances the activity of glutamate transporters GLAST, GLT1 and EAAC1. *Eur J Pharmacol* **578**, 171-176 (2008).
37. M. Carbone, S. Duty, M. Rattray, Riluzole elevates GLT-1 activity and levels in striatal astrocytes. *Neurochem Int* **60**, 31-38 (2012).
38. A. C. Pereira *et al.*, Age and Alzheimer's disease gene expression profiles reversed by the glutamate modulator riluzole. *Mol Psychiatry* **22**, 296-305 (2017).
39. H. C. Hunsberger *et al.*, Riluzole rescues glutamate alterations, cognitive deficits, and tau pathology associated with P301L tau expression. *J Neurochem* **135**, 381-394 (2015).
40. J. D. Rothstein, L. J. Martin, R. W. Kuncl, Decreased glutamate transport by the brain and spinal cord in amyotrophic lateral sclerosis. *N Engl J Med* **326**, 1464-1468 (1992).
41. J. D. Rothstein, M. Van Kammen, A. I. Levey, L. J. Martin, R. W. Kuncl, Selective loss of glial glutamate transporter GLT-1 in amyotrophic lateral sclerosis. *Ann Neurol* **38**, 73-84 (1995).
42. J. R. Tollervey *et al.*, Characterizing the RNA targets and position-dependent splicing regulation by TDP-43. *Nat Neurosci* **14**, 452-458 (2011).
43. M. R. Jablonski *et al.*, Inhibiting drug efflux transporters improves efficacy of ALS therapeutics. *Ann Clin Transl Neurol* **1**, 996-1005 (2014).
44. L. A. Mohamed, S. S. Markandaiah, S. Bonanno, P. Pasinelli, D. Trotti, Excess glutamate secreted from astrocytes drives upregulation of P-glycoprotein in endothelial cells in amyotrophic lateral sclerosis. *Exp Neurol* **316**, 27-38 (2019).